Journal of Catalysis **198,** 277–285 (2001)
doi:10.1006/jcat.2000.3151, available online at http://www.idealibrary.com on IDEAL®

Monoclinic and Tetragonal High Surface Area Sulfated Zirconias in Butane Isomerization: CO Adsorption and Catalytic Results

W. Stichert,*,[1] F. Schüth,* S. Kuba,† and H. Knözinger†

**MPI für Kohlenforschung, Kaiser-Wilhelm-Platz 1, D-45470 Mülheim, Germany; and †Department Chemie, Physikalische Chemie, Universität München, Butenandtstrasse 5-13 (Haus E), 81377 Munich, Germany*

Received August 24, 2000; revised December 6, 2000; accepted December 12, 2000; published online February 15, 2001

In the present study high surface area monoclinic and tetragonal sulfated zirconia samples both active in *n*-butane isomerization were prepared from the same hydroxide precursor in a novel one-step hydrothermal process. The process is studied via analysis of intermediate stages of the product formation. The monoclinic samples show a catalytic activity in *n*-butane isomerization lower by about a factor of 4 compared to the tetragonal samples, although the acidity as analyzed by CO adsorption was found to be similar. This suggests, that it is not only the acidity of sulfated zirconia that determines the catalytic performance. The results support the bimolecular mechanism, for which a favorable arrangement of surface groups is necessary. The surface structure of tetragonal zirconia seems to be better suited than that of the monoclinic zirconia, although the presented monoclinic zirconia performs substantially better than claimed in many publications, where the monoclinic phase is typically assumed to be inactive. © 2001 Academic Press

Key Words: **zirconia; monoclinic; tetragonal; butane isomerization; CO adsorption.**

INTRODUCTION

Catalytic properties of sulfated zirconia were first described by Holm and Bailey in 1962 (1). However, there was no specific interest in this material until 1979 when Arata *et al.* reported the activity of sulfated zirconia for *n*-butane isomerization at room temperature (2). Since that time the properties of sulfated zirconia and its potential use in acid-catalyzed reactions, especially in *n*-butane isomerization, have been investigated and discussed extensively.

Despite numerous investigations, current research on sulfated zirconia is still focused on basic aspects, e.g., the nature of its active sites (3–6) and the reaction mechanism (7–11). The acid site strength of sulfated zirconia is also one of the aspects discussed. In earlier publications sulfated zirconia was considered a solid superacid (2, 12), which was thought to be the reason for its activity in *n*-butane isomerization. However, this was based on the assumption of a monomolecular reaction mechanism that requires very strong acid sites. Recent publications revealed that the isomerization of *n*-butane with sulfated zirconia proceeds via a bimolecular mechanism, possibly involving C_8^+ ions. This mechanism does not necessarily require a superacid catalyst (7, 8). These results are also in agreement with the experimental observation and computations that the acid sites of sulfated zironia are weaker than acid sites of HZSM-5 (4, 13–15). This led to the conclusion that the activity of sulfated zirconia may be due to its ability to stabilize a transition state complex of the organic reactants on the surface (4).

The occurrence of such a transition state complex implies the existence of a certain optimized geometrical arrangement on the surface of highly active sulfated zirconia. This is one reason why even in recent publications a good catalytic activity is considered to be connected to tetragonal zirconia (16–19). Also the activity of an X-ray amorphous sulfated zirconia was attributed to very small tetragonal domains (20). With respect to the monoclinic phase, for a long time it was not possible to prepare a catalytically active monoclinic material, because sulfate on the surface of zirconia stabilizes the crystallite size of zirconia upon calcination and therefore its tetragonal crystal phase (21) up to temperatures at which the sulfate already leaves the surface. Therefore, in the first attempts to prepare active monoclinic sulfated zirconia, a crystalline precursor, first calcined at higher temperatures to induce the tetragonal–monoclinic phase transition, was impregnated with sulfuric acid. However, the resulting materials did not exhibit high activity (22–24). A moderate activity of precalcined monoclinic zirconia was achieved by applying very drastic sulfation conditions (25). Recently, Morterra *et al.* prepared a mainly monoclinic material with an activity similar to that of their corresponding purely tetragonal sulfated zirconias by varying the sulfur content of their samples (26, 27). However, this material prepared by an aerogel procedure still exhibited a tetragonal phase content of 30%, which made it difficult to attribute the activity to the monoclinc phase alone. We recently reported a two-step method for the preparation of purely monoclinic sulfated zirconia with

---

[1] Present address: hte AG, Kurpfalzring 104, 69123 Heidelberg, Germany.

0021-9517/01 $35.00

an activity in *n*-butane isomerization in the same order of magnitude as the corresponding tetragonal materials (28).

However, the existence of a catalytically active monoclinic sulfated zirconia does not necessarily contradict the theory of the transition state complex. It has been reported, based on infrared (IR) spectroscopy and CO adsorption, that sulfation of zirconia leads to a major change in its surface properties, especially with respect to the binding character of the present hydroxyl groups (24, 29), irrespective of the phase of zirconia. An alteration of the surface geometry caused by sulfation of monoclinic zirconia in the same or at least similar manner as for tetragonal zirconia therefore seems to be possible. A different bulk phase does not inevitably result in totally different surface properties, as surface reconstruction might occur, especially under the influence of an adsorbate such as sulfate. Such surface properties of zirconia can be assessed with IR spectroscopy coupled with CO adsorption at low temperatures, which has been widely accepted as a valuable tool for such analyses (13, 24, 29, 30–34).

Many preparation methods for sulfated zirconia have been reported in the literature. Most of them concern the classical two-step method (2, 12), which consists of the synthesis of an amorphous zirconium hydroxide precursor and its impregnation with sulfuric acid or ammonium sulfate. An alternative is the one-step sol–gel synthesis, to which many of the recent publications are devoted (26, 27, 35, 36).

In this paper we address the following points:

(i) We report a new one-step crystallization method that leads to catalytically active monoclinic sulfated zirconia.

(ii) We investigate the effect of hydrothermal aging of a zirconium oxide precursor by physicochemical characterization of the intermediate products of this aging process and measuring the catalytic activities of the resulting oxides.

(iii) We analyze the surface properties of the resulting active monoclinic sulfated zirconia by means of IR spectroscopy and CO adsorption at 77 K in order to elucidate the connection between the crystalline phase and the activity in *n*-butane isomerization of sulfated zirconia.

EXPERIMENTAL

Synthesis

The sulfated zirconia samples were prepared in the following way: 20 g of $ZrOCl_2 * 8H_2O$ (ABCR, 95%) was dissolved in 200 ml of deionized water and stirred for 5 min. An aqueous solution of NH_4OH (Roth, ≥25%) was added to reach a pH of 1.2. After stirring for 7 min 30 s, 2.64 g of $(NH_4)_2SO_4$ (Fluka, 99%) was added. The stirring was continued for another 2 h. Subsequently, the resulting mixture was divided in five parts. Because it was difficult to filter off the precipitate, the excess solution of the first part was decanted and the remaining solid was dried at 363 K for 24 h. Obviously, some ammonium sulfate will remain in the solid by applying this method. The other four solutions were aged for 2, 4, 6, and 20 h, respectively, in an autoclave at 423 K. These solutions were also decanted and the resulting solids were dried at 363 K for 24 h. Finally, all resulting sulfated hydrous zirconias were calcined for 5 h at 823 K, with a heating rate of 1 K/min. These or similar procedures were repeated several times with similar results. However, here we report only one set of data measured for samples from the very same master batch. The non-aged calcined sample is referred to as SZ-1 in the following; the other samples, SZ-2 to SZ-5, correspond to the increasing aging times.

Sample Characterization

The X-ray diffraction (XRD) patterns were recorded using a Stoe STADI P diffractometer equipped with a Germanium monochromator in transmission geometry. The diffractograms were measured within the range of 27° to 34.5° (2Θ) using Cu$K\alpha$ radiation. The crystallite sizes were calculated by means of a procedure contained in the Stoe Visual X^{POW} software package, the single line size/strain Fourier analysis. Due to the fact that only one X-ray reflection with relatively low intensity could be analyzed, the error of this method is rather high and lies in the range of ±30%. But even if the absolute size cannot be measured correctly, these values can be used for a comparison between the samples.

The nitrogen adsorption–desorption isotherms were measured at 77 K with a Micromeritics ASAP 2010 system. Prior to the measurements the samples were outgassed for 4 h at 413 K. The specific surface areas of all samples were calculated according to the BET method (37). The thermogravimetric (TG) measurements were carried out using a Setaram TG-DTA 92-16. The samples were heated continuously with a rate of 10 K/min from 288 to 1273 K in a static air atmosphere.

The IR spectra were recorded with a Bruker IFS-88 FTIR spectrometer equipped with a liquid nitrogen cooled MCT detector. The spectral resolution was 2 cm^{-1}. An *in situ* transmission cell (38) was used for low temperature IR spectrometric studies. The samples were prepared as thin self-supporting wafers (15–20 mg/cm^2), which were first activated at 673 K for 1 h in an oxygen flow. Subsequently, the sample was evacuated for 1 h at 673 K. The spectra were recorded at 77 K after exposure to increasing equilibrium pressures of CO (0.1–5 hPa).

Catalytic Testing

The catalytic properties of the samples (as powder on quartz wool) were studied for *n*-butane isomerization in a fixed-bed flow reactor (inner diameter = 8 mm) with external heating at 573 K. The zirconia (0.5 g) was exposed to a 50 : 50 vol% mixture of *n*-butane and nitrogen with a constant feed of 10 ml/min. The reaction products were analyzed with a Carlo Erba GC6000 equipped with a DB-5 column and a flame ionization detector. Prior to the measurement the samples were activated at 723 K for 2 h under a constant nitrogen flow of 20 ml/min. No further change of the phase composition was observed during such a treatment for either of the samples.

RESULTS

Figure 1a shows the XRDs of the calcined samples. The diffractogram of SZ-1 contains almost exclusively the tetragonal phase. This is an expected result, since the preparation procedure of this sample is quite similar to the well-known and well-reported classical method. The XRDs of the samples with the aged precursors show clearly how the phase composition of calcined zirconia changes after aging of the precursor: The content of the monoclinic phase increases until, after 20 h of aging, the resulting sulfated zirconia sample is purely monoclinic. Figure 1b shows a diffractogram of SZ-5 in the range between 5° (2Θ) to 80° (2Θ). The diffractogram shows a purely monoclinic phase, and a very small crystallite size can be calculated. The diffraction patterns of samples were also measured before calcination (Fig. 1c). The precursors of SZ-1, SZ-2, and SZ-3 are totally X-ray amorphous—the strong reflection at about 32.5° (2Θ) belongs to crystalline ammonium sulfate, the precursor of SZ-4 exhibits a very small fraction of the monoclinic phase, and the XRD of the precursor of SZ-5 is similar to the XRD of the corresponding calcined sample. This clearly indicates a crystallization process from amorphous to monoclinic hydrous zirconia during the hydrothermal aging. The amorphous precipitate crystallizes upon calcination and results in the tetragonal phase whereas the crystallized monoclinic hydrous zirconia results in monoclinic zirconia. This is in accordance with the thermodynamic data as the monoclinic phase is the thermodynamically more stable phase for bulk zirconia between room temperature and about 1500 K. From line broadening analysis of the X-ray reflections the crystallite size was calculated to be approximately 12 nm for the tetragonal sample SZ-1, while a value of only ca. 5 nm was obtained for the monoclinic sample SZ-5 (Table 1).

TABLE 1

Crystallite Size and Particle Size Calculated from XRD and BET Surface Area, Respectively, of the Tetragonal and the Monoclinic Samples

Sample	Crystallite size (nm)	Particle size (nm)
SZ-1	12 (tet)	12
SZ-5	5 (mon)	7

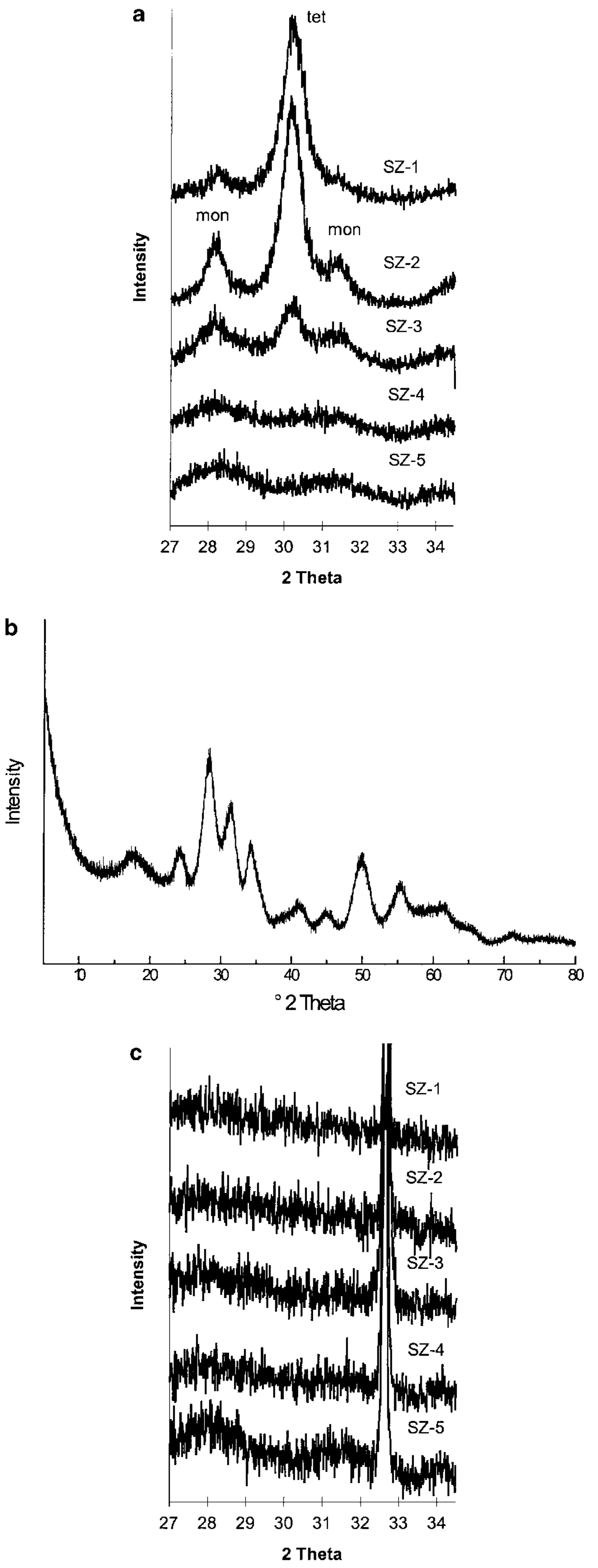

FIG. 1. (a) Diffractograms of the samples calcined for 5 h at 823 K with a heating rate of 1 K/min. (b) Diffractogram of SZ-5 measured over night in the 2Θ range beween 5° and 80°. (c) Diffractograms of the noncalcined samples.

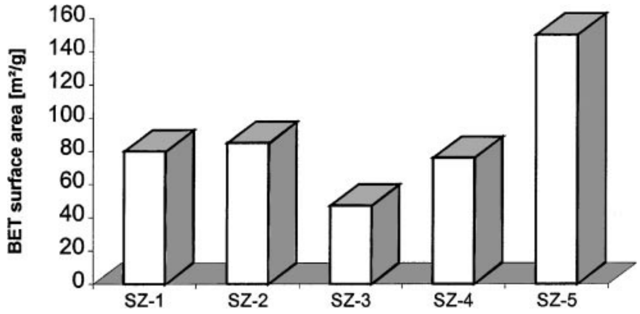

FIG. 2. BET surface areas of the calcined samples.

TABLE 2

Thermal Weight Loss of the Calcined Samples in the Water and Sulfate Regime, Respectively

	Weight loss (%)	
Sample	293–473 K	873–1023 K
SZ-1	2.6	2.4
SZ-2	2.6	2.4
SZ-3	2.4	8
SZ-4	3.9	6.7
SZ-5	5.1	4.8

Figure 2 shows the BET surface areas calculated from the nitrogen adsorption–desorption isotherms of the calcined samples. Of particular interest are the BET surface areas of SZ-1 (80 m^2/g) and SZ-5 (150 m^2/g). Assuming a spherical shape of the particles, it is possible to calculate the particle sizes of the samples. Table 1 shows that the calculated values are in very good agreement with the crystallite sizes of the samples determined from XRD line broadening, suggesting that a large fraction of SZ-5 is indeed present as such small monoclinic crystallites.

Figure 3 shows the TG curves of the calcined samples; Table 2 shows the corresponding weight losses of the samples occurring in two pronounced steps between room temperature and 473 K and between 873 and 1023 K, respectively. The first weight loss is assigned to the loss of physisorbed water, the second one to the loss of sulfate groups. The additional weight loss notable as a slope of the TG curves and occurring basically over the entire temperature range can be attributed to water resulting from dehydroxylation of the hydrous zirconia. The attribution of the second weight loss between 873 and 1023 K to sulfur was confirmed by additional TG/mass spectroscopy experiments, where the masses corresponding to SO_2 and its fragmentation products were for all five samples the only changes detected in the mass spectroscopy concurrent with the TG mass losses. These losses can thus be used to estimate the sulfate content of the samples. Normalized to the surface area, the sulfate contents of purely tetragonal sample SZ-1, the predominantly tetragonal SZ-2, and the purely monoclinic sample SZ-5 seem to be quite similar (approximately 3 μmol SO_4^{2-}/m^2). The same holds for the water content of these two samples. In contrast, SZ-4 and especially SZ-3 exhibit much lower surface areas and higher sulfate contents, suggesting that sulfate is located also in the bulk of these recrystallization intermediates.

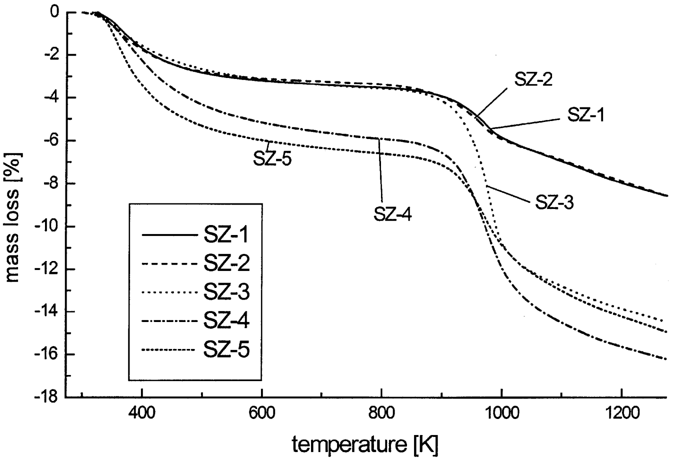

FIG. 3. Thermal weight loss of the calcined samples in the temperature range between 293 and 1273 K.

Figure 4a shows the rate of *n*-butane conversion vs time-on-stream of the samples normalized to the mass of the catalyst. The initial specific rates for SZ-1, SZ-2, and SZ-5 are very similar and somewhat higher than those for SZ-3 and SZ-4. All samples deactivate during the first 5 h before they reach an almost stationary activity. The steepest activity decay within the first hour on stream is seen for SZ-5. The stationary activities are almost identical for SZ-3, SZ-4, and SZ-5 and about one third of those observed for samples SZ-1 and SZ-2.

This difference becomes even more pronounced when the activity is not normalized to mass but to surface area: Fig. 4b shows the corresponding catalytic data of the samples. Here, the materials fall into three different groups: in the regime of stationary activities SZ-1 and SZ-2 exhibit the highest specific rate, followed by SZ-3 and SZ-4 at an intermediate specific rate while SZ-5 shows the lowest activity. SZ-1 exhibits an initial rate two times higher and after 10 h a rate five times higher than that of SZ-5. After 10 h SZ-1 retains about 25% of its intitial rate, SZ-5 only about 11%. The monoclinic sample therefore shows a lower specific rate and a faster deactivation than the tetragonal sample. Selectivities are well above 95% in all cases.

In an attempt to correlate these differences with the acidities of the samples, the monoclinic sample was analyzed using CO adsorption followed by IR spectroscopy. Figure 5 shows the hydroxyl stretching region (3300–3800 cm^{-1}) of the monoclinic sulfated zirconia sample. CO was adsorbed at ca. 85 K by a stepwise increase of the CO pressure from

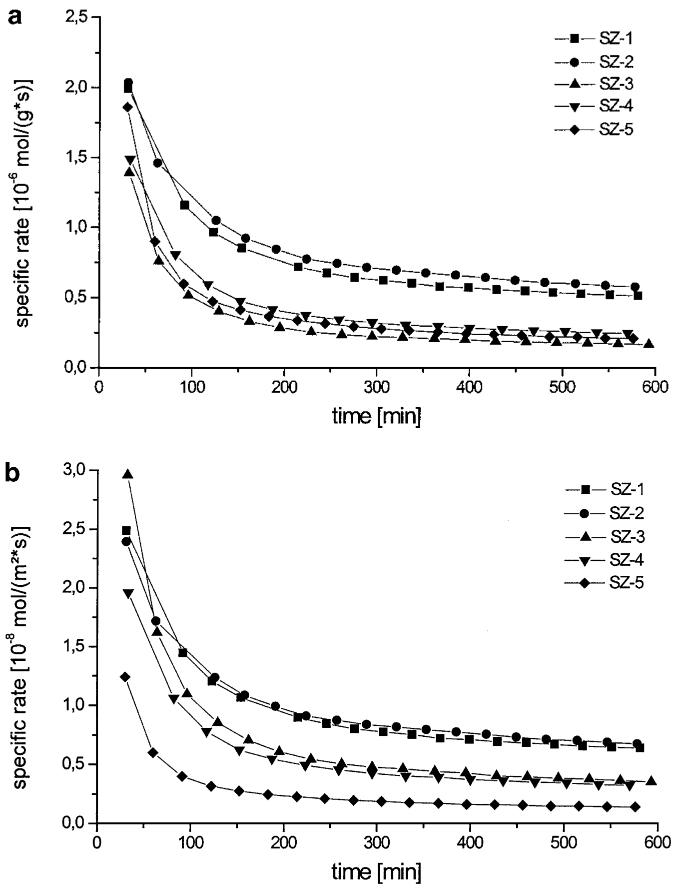

FIG. 4. (a) Specific rate in *n*-butane isomerization of the samples normalized to the mass. (b) Specific rate in *n*-butane isomerization of the samples normalized to the surface area.

0.5 to 5 hPa (spectra b–k). Spectrum a shows the hydroxyl stretching region of the sample prior to CO adsorption. A band at 3640 cm^{-1} and another weak ν_{OH} band at about 3580 cm^{-1} can be seen. In addition, a broad unstructured absorption band is visible over the entire OH-stretching frequency range. Increasing CO pressure leads to a decrease in the intensity of the band at 3640 cm^{-1} and the simultaneous formation of a new band at 3480 cm^{-1}, which corresponds to a $\Delta\nu_{OH}$ of about -160 cm^{-1}. The band at 3580 cm^{-1} is not affected by CO adsorption. At higher CO pressures a new band at 3705 cm^{-1} forms.

Figure 6 shows the carbonyl stretching region (2100–2250 cm^{-1}) of the IR spectra of the monoclinic sample, plotted analogously to Fig. 5. At low CO pressures, first a band at 2202 cm^{-1} appears. A second band at 2198 cm^{-1} develops with increasing pressure. At a pressure of 0.3 hPa CO an additional band at 2170 cm^{-1} appears, which is also shifted to lower wavenumbers with increasing pressure.

The region of the spectra with characteristic S=O bands (1200–1500 cm^{-1}) is plotted in Fig. 7. Without adsorbed CO a band at 1394 cm^{-1} with a shoulder at 1402 cm^{-1} appears. At low CO pressures these bands shift to 1380 cm^{-1} and

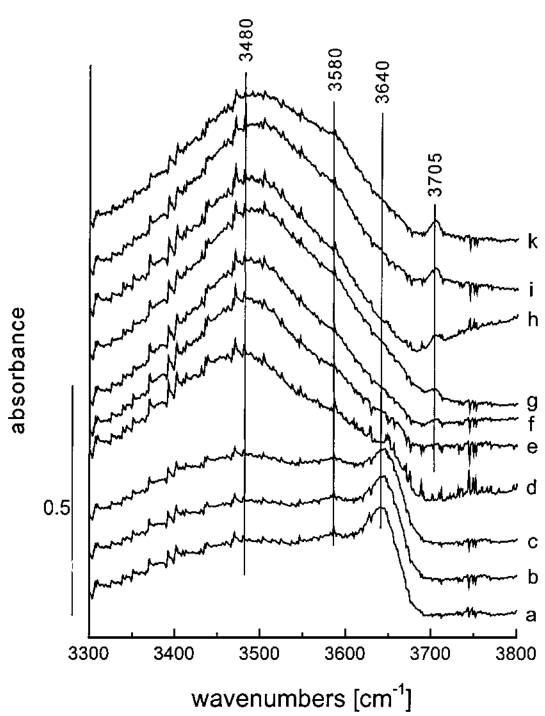

FIG. 5. IR spectra of the monoclinic sample in the hydroxyl stretching region (a) without any adsorbed CO and with (b) 0.1 hPa, (c) 0.2 hPa, (d) 0.3 hPa, (e) 0.4 hPa, (f) 0.5 hPa, (g) 1.0 hPa, (h) 1.5 hPa, (i) 2.0 hPa, and (k) 5.0 hPa CO adsorbed.

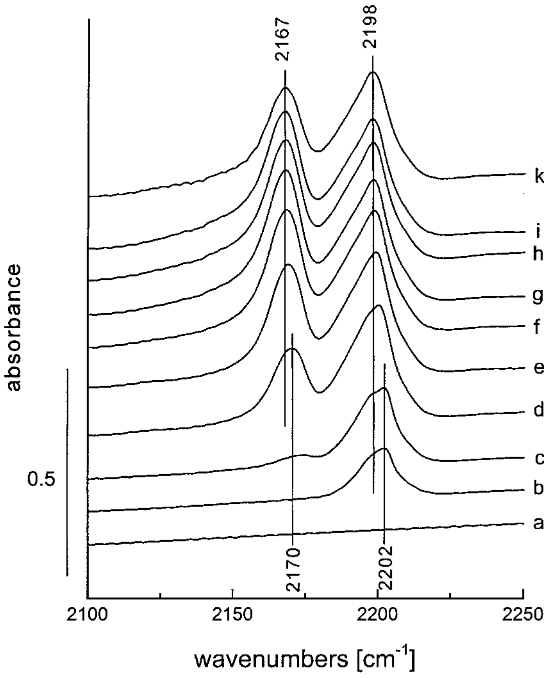

FIG. 6. IR spectra of the monoclinic sample in the carbonyl stretching region (a) without any adsorbed CO and with (b) 0.1 hPa, (c) 0.2 hPa, (d) 0.3 hPa, (e) 0.4 hPa, (f) 0.5 hPa, (g) 1.0 hPa, (h) 1.5 hPa, (i) 2.0 hPa, and (k) 5.0 hPa CO adsorbed.

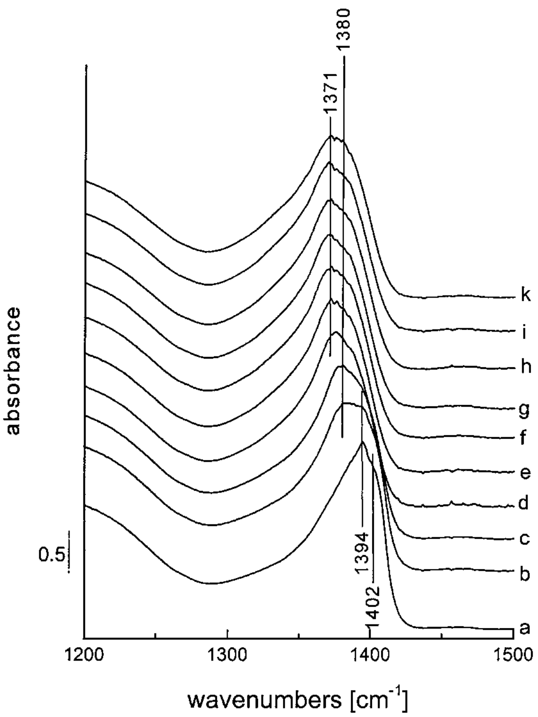

FIG. 7. IR spectra of the monoclinic sample in the sulfate region (a) without any adsorbed CO and with (b) 0.1 hPa, (c) 0.2 hPa, (d) 0.3 hPa, (e) 0.4 hPa, (f) 0.5 hPa, (g) 1.0 hPa, (h) 1.5 hPa, (i) 2.0 hPa, and (k) 5.0 hPa CO adsorbed.

at higher pressures to 1371 cm^{-1}. The band at 1380 cm^{-1} is still present as a shoulder at higher pressures.

DISCUSSION

Before the results are discussed in detail, it seems important to compare the resulting material and the synthesis procedure with the existing literature. In 1964, Clearfield first described the formation of crystalline (monoclinic) hydrous zirconia by refluxing a $ZrOCl_2 * 8H_2O$ solution (39). Later on, he extended this method by varying the pH of the refluxed solution and reported the formation of also tetragonal hydrous zirconia (40). Many publications concerning these materials have appeared, especially with respect to ceramic applications (41, 42). It has also been described that it is possible to shorten the crystallization time by applying higher temperatures and carrying out the process in an autoclave (43, 44). What is referred to here as "aging at 423 K" is similar to this recrystallization process. The main difference in the procedure applied in this study is the presence of sulfate during the crystallization process to lead directly to sulfated hydrous zirconia. Recently, a series of papers appeared concerning a "digestion" of amorphous hydrous zirconia samples (45–48). This "digestion" is also equivalent to the "aging" process applied in this study and the recrystallization process described first by Clearfield in the 60s.

However, the results in the present paper indicate a crystallization of hydrous zirconia under hydrothermal conditions in the presence of sulfate groups, which leads after a calcination step to a sulfated zirconia catalyst that is active in *n*-butane isomerization. Since the sulfate groups stabilize the particle size upon calcination and no substantial growth will occur during thermal treatment, the crystallite sizes reflect the situation after aging. The particle sizes thus suggest that during crystallization of the amorphous zirconium hydroxide after a short period of particle growth small crystallites of zirconia form that soon cease to grow. Calcination of the sulfated hydroxides/hydrous zirconias results in the formation of sulfated zirconias with a continuous spectrum of phase compositions, depending on the aging time.

Of special interest are the purely tetragonal and the purely monoclinic samples, SZ-1 and SZ-5, respectively. These samples differ in specific surface area, physisorbed water content, and sulfate content by a factor of about 2. Assuming that all sulfate and physisorbed water is located on the surface (a rough calculation shows that the surface can accommodate such amounts of adsorbed species), an approximately similar concentration of these species on the surfaces of the two samples can be inferred.

This information is helpful to judge the catalytic performance of the samples. The monoclinic sample should consequently exhibit an activity normalized to the surface area similar to that of the tetragonal sample, if the concentration of the sulfate groups were the only decisive factor. As it is clearly shown, this is not the case: the monoclinic sulfated zirconia has the lowest catalytic initial and stationary activity of all samples tested (see Fig. 4). However, contrary to what is often claimed in the literature, it is not inactive, but has an activity at least on the same order of magnitude as the tetragonal sample. One should note here that more active tetragonal zirconias could be produced by optimizing the preparation conditions. For example, a higher pH at the precipitation step produces more active catalysts (49, 50). However, conditions optimized for the production of a most active tetragonal zirconia could not be used, since monoclinic hydrous zirconia cannot be obtained via the recrystallization process any more (6). It seemed more important in this comparative study to keep the preparation of the samples as similar as possible. However, the calcination temperature, which is also important (51–53), is optimized with respect to catalytic activity both for the tetragonal and the monoclinic sample: In a separate set of experiments the calcination temperature that results in the formation of the most active catalysts was determined and found to be 823 K.

An IR study coupled with CO adsorption at 77 K was undertaken to check whether the acidic properties of the monoclinic sulfated zirconia sample are different from the acidic properties of tetragonal samples.

Hydroxyl Stretching Region

The sulfated sample without any adsorbed CO shows a band at 3640 cm^{-1}. This band is assigned to a bridging hydroxyl group in the literature (24) and is observed, with small variations in the exact position, for all sulfated zirconia samples reported in the literature. Spielbauer *et al.* (24) have measured a monoclinic sulfated zirconia sample, which, however, was catalytically inactive. They also observed the band at 3640 cm^{-1}. After CO adsorption this band shifts to a broad band at about 3480 cm^{-1}, which corresponds to a $\Delta\nu_{OH}$ value of about -160 cm^{-1}. This value is exactly the same as that reported for sulfated active tetragonal and sulfated inactive monoclinic zirconia (24). Therefore, the occurrence of this band at 3640 cm^{-1} and its shift to 3480 cm^{-1} upon CO adsorption cannot be taken as a measure for the activity of sulfated zirconia in *n*-butane isomerization. The hydroxyl stretching region of unsulfated zirconia, however, is different (24). This suggests that sulfate groups modify the surface of tetragonal and monoclinic zirconia in a similar way with respect to the hydroxyl groups and that the presence of such groups is probably a necessary, but not sufficient, condition for activity in *n*-butane isomerization. The monoclinic sample exhibits two additional very weak bands at 3580 and 3705 cm^{-1}. The band at 3580 cm^{-1} does not seem to be affected by CO uptake. This band has already been observed before on sulfated zirconia (54). Since it is not present on pure zirconia samples this band was assigned to OH-containing species, whose presence is related to the presence of surface sulfates. The origin of the weak band at 3705 cm^{-1} is not known at present.

Carbonyl Stretching Region

The carbonyl stretching region of the spectra shows two bands, one at 2202 cm^{-1} and one at 2198 cm^{-1}. The band at 2202 cm^{-1} is present already at low CO coverages while the band at 2198 cm^{-1} grows in at higher coverages. These frequencies are typical for CO adsorbed on Zr^{4+} centers (Lewis acid centers). The occurrence of the two bands suggests the presence of two types of Lewis acid sites having different acid site strength. At a pressure of 0.3 hPa CO an additional band at 2170 cm^{-1} appears that is shifted to 2167 cm^{-1} upon higher loadings. This band is due to CO bonded to OH groups. Spielbauer *et al.* (24) observed the same bands (CO coordinated to Zr^{4+} centers and H bonded to OH groups) both on monoclinic inactive sulfated zirconia and on tetragonal active sulfated zirconia. In addition, they observed a difference in the relative intensities of the bands on these two samples: Whereas the inactive monoclinic sample showed just a low intensity of the bands at 2200 cm^{-1} compared to the intensities of the bands at 2170 cm^{-1}, the active tetragonal sample shows almost equal intensities of these two bands. They suggested a relationship between the relative intensity of these two bands and the activity of the materials in *n*-butane isomerization. The monoclinic material investigated in this study also shows almost equal intensities for both kinds of bands and is thus very similar to active tetragonal zirconia, such as the tetragonal material reported by Spielbauer *et al.* (24). The results suggest that an optimal balance between Lewis and Brønsted acid site densities is required for the reaction. The intensity ratio of the bands in the CO stretching region can thus be used to discriminate between inactive and active zirconias, but it is not possible to differentiate between materials where the catalytic activities are in the same order of magnitude.

Sulfate Region

The spectrum of the sample in the absence of CO shows a band at 1394 cm^{-1} with a shoulder at 1402 cm^{-1}. At low CO pressure these bands already shift to lower wavenumbers and they appear at 1371 and 1380 cm^{-1}, respectively, at the highest CO pressures investigated. These bands belong to S=O groups. The shift of these bands is due to both the adsorption of CO on Lewis acid sites and on OH groups (24). The positions of these bands resemble the band positions reported in the literature for the S=O groups. The shift of these bands is also in the same order of magnitude as previously reported for tetragonal sulfated zirconia.

Therefore, it can be concluded that no major difference in the spectra—and thus the acidity—between the monoclinic sample investigated in this study and tetragonal samples prepared via the classical synthesis route can be observed, although catalytic activity differs by a factor of 2 to 5, depending on time-on-stream. These results are therefore in line with the findings of other publications concerning the mechanism of the reaction as a bimolecular reaction. In order to optimally stabilize a C_8-intermediate the appropriate arrangement of surface groups will be needed. It is thus not primarily the acidity of the surface—although a certain acid site strength will be needed—but also the surface structure that will influence the catalytic activity in *n*-butane isomerization. Contrary to what is reported in many publications, however, the surface structure of monoclinic zirconia is obviously not so unfavorable as to render monoclinic sulfated zirconias inactive. To synthesize monoclinic sulfated zirconia with a catalytic activity on the same order as tetragonal sulfated zirconia, one has to find suitable pathways for the synthesis of monoclinic zirconias with a sufficiently high surface area to result in measurable activity and a sufficiently high sulfate group concentration on the surface. Converting just sulfated tetragonal zirconia to the monoclinic phase is not a suitable pathway, since this results in low surface area monoclinic zirconia on the one hand and leads to decomposition of the surface sulfate groups on the other hand.

CONCLUSIONS

The data presented clearly demonstrate that it is possible to synthesize catalytically active monoclinic sulfated zirconia in one step by means of a hydrothermal crystallization process. Therefore, the occurrence of catalytic activity in *n*-butane isomerization of the samples cannot be connected with the tetragonal phase of zirconia alone. The hydrothermal process under the conditions applied in this study produces a monoclinic hydrous zirconia precursor that leads after calcination to a material with a high surface area (150 m^2/g). The acidic properties measurable by CO adsorption and IR spectroscopy of the resulting monoclinic sample are not discerniable from the properties of tetragonal samples. A possible explanation is that the sulfation process modifies the surface of zirconia independently of the bulk phase and thus results in a similar structure at the immediate sulfate site. However, the arrangement of surface groups on a larger scale can differ nevertheless. Therefore, a mechanism of the isomerization reaction involving the stabilization of a transition state complex of a bimolecular reaction, in which a larger fraction of the surface would be involved, seems feasible. A connection between the catalytic activity of sulfated zirconias and different surface phases (55) seems not to be supported by the results presented here.

The data also show that IR spectroscopy coupled with CO adsorption alone cannot be applied as a measure for the activity of sulfated zirconia. The monoclinic sample clearly shows catalytic properties inferior to those of the tetragonal sample, which cannot be explained by the spectroscopic results. It therefore seems indeed necessary to measure the catalytic performance for each synthesized sample, since no clear correlation between a physicochemical property and the activity can be identified, yet.

ACKNOWLEDGMENTS

We thank Klaus Schlichte for repeating some of the experiments. The work was supported by the Fonds der Chemischen Industrie. In addition, the work done in Munich was financially supported by the Deutsche Forschungsgemeinschaft (SFB 338).

REFERENCES

1. Holm, V. C. F., and Bailey, G. C., US Patent 3 032 599, 1962.
2. Hino, M., Kobayashi, S., and Arata, K., *J. Am. Chem. Soc.* **101**, 6439 (1979).
3. Song, S. X., and Kydd, R. A., *J. Chem. Soc. Faraday Trans.* **94**(9), 1333 (1998).
4. Adeeva, V., de Haan, J. W., Jänchen, J., Lei, G. D., Schünemann, V., van de Ven, L. J. M., Sachtler, W. M. H., and van Santen, R. A., *J. Catal.* **151**, 364 (1995).
5. Arata, K., and Hino, M., *Mater. Chem. Phys.* **26**, 213 (1990).
6. Clearfield, A., Serrette, G. P. D., and Khazi-Syed, A. H., *Catal. Today* **20**, 295 (1994).
7. Adeeva, V., Lei, G. D., and Sachtler, W. M. H., *Catal. Lett.* **33**, 135 (1995).
8. Liu, H., Adeeva, V., Lei, G. D., and Sachtler, W. M. H., *J. Mol. Catal. A: Chem.* **100**, 35 (1995).
9. Fogash, K. B., Larson, R. B., González, M. R., Kobe, J. M., and Dumesic, J. A., *J. Catal.* **163**, 138 (1996).
10. Suzuku, T., and Okuhara, T., *Chem. Lett.* 470 (2000).
11. Matsushita, H., Shibata, H., Nakamura, H., and Arata, K., *Appl. Catal. A—Gen.* **187**, 99 (1999).
12. Hino, M., and Arata, K., *J. Chem. Soc. Chem. Commun.* 851 (1980).
13. Kustov, L. M., Kazansky, V. B., Figueras, F., and Tichit, D., *J. Catal.* **150**, 143 (1994).
14. Drago, R. S., and Kob, N., *J. Phys. Chem. B* **101**, 3360 (1997).
15. Haase, F., and Sauer, J., *J. Am. Chem. Soc.* **120**, 13,503 (1998).
16. Farcasiu, D., Li, J. Q., and Cameron, S., *Appl. Catal. A—Gen.* **154**, 173 (1997).
17. Farcasiu, D., and Li, J. Q., *Appl. Catal. A—Gen.* **128**, 97 (1995).
18. Comelli, R. A., Vera, C. R., and Parera, J. M., *J. Catal.* **151**, 96 (1995).
19. Chen, F. R., Coudurier, G., Joly, J.-F., and Vedrine, J. C., *J. Catal.* **143**, 616 (1993).
20. Risch, M. A., and Wolf, E. E., *Appl. Catal. A—Gen.* **172**, L1 (1998).
21. Stichert, W., and Schüth, F., *Chem. Mater.* **10**, 2020 (1998).
22. Ward, D. A., and Ko, E. I., *J. Catal.* **157**, 321 (1995).
23. Morterra, C., Cerrato, G., Pinna, F., and Signoretto, M., *J. Catal.* **157**, 109 (1995).
24. Spielbauer, D., Mekhemer, G. A. H., Zaki, M. I., and Knözinger, H., *Catal. Lett.* **40**, 71 (1996).
25. Vera, C. R., and Parera, J. M., *J. Catal.* **165**, 254 (1997).
26. Morterra, C., Cerrato, G., Di Ciero, S., Signoretto, M., Pinna, F., and Strukul, G., *J. Catal.* **165**, 172 (1997).
27. Signoretto, M., Pinna, F., Strukul, G., Chies, P., Cerrato, G., Di Ciero, S., and Morterra, C., *J. Catal.* **167**, 522 (1997).
28. Stichert, W., and Schüth, F., *J. Catal.* **174**, 242 (1998).
29. Morterra, C., Cerrato, G., and Di Ciero, S., *Appl. Surf. Sci.* **126**, 107 (1998).
30. Scheithauer, M., Grasselli, R. K., and Knözinger, H., *Langmuir* **14**, 3019 (1998).
31. Morterra, C., Cerrato, G., and Signoretto, M., *Catal. Lett.* **41**, 101 (1996).
32. Morterra, C., Cerrato, G., Bolis, V., Di Ciero, S., and Signoretto, M., *J. Chem. Soc. Faraday Trans.* **93**, 1179 (1997).
33. Spielbauer, D., Mekhemer, G. A. H., Riemer, T., Zaki, M. I., and Knözinger, H., *J. Phys. Chem. B* **101**, 4681 (1997).
34. Morterra, C., Cerrato, G., and Pinna, F., *Spectrochim. Acta A* **55**, 95 (1999).
35. Tichit, D., Coq, B., Armendariz, H., and Figuéras, F., *Catal. Lett.* **38**, 109 (1996).
36. Li, B., and Gonzalez, R. D., *Ind. Eng. Chem. Res.* **35**, 3141 (1996).
37. Brunauer, S., Emmett, P. H., and Teller, E., *J. Am. Chem. Soc.* **60**, 309 (1938).
38. Kunzmann, G., Dissertation, University of Munich, 1987.
39. Clearfield, A., *Inorg. Chem.* **3**, 146 (1964).
40. Clearfield, A., *J. Mater. Res.* **5**, 161 (1990).
41. Matsui, K., Suzuki, H., Ohgai, M., and Arashi, H., *J. Am. Ceram. Soc.* **78**, 146 (1995).
42. Matsui, K., and Ohgai, M., *J. Am. Ceram. Soc.* **80**, 1949 (1997).
43. Nishizawa, H., Yamasaki, N., Matsuoda, K., and Mitsushio, H., *J. Am. Ceram. Soc.* **65**, 343 (1982).
44. Bucko, M. M., Haberko, K., and Faryna, M., *J. Am. Ceram. Soc.* **78**, 3397 (1995).

45. Chan, K. S., Chuah, G. K., and Jaenicke, S., *J. Mater. Sci. Lett.* **13**, 1579 (1994).
46. Chuah, G. K., Jaenicke, S., Cheong, S. A., and Chan, K. S., *Appl. Catal. A—Gen.* **145**, 267 (1996).
47. Chuah, G. K., and Jaenicke, S., *Appl. Catal. A—Gen.* **163**, 261 (1997).
48. Chuah, G. K., Jaenicke, S., and Pong, B. K., *J. Catal.* **175**, 80 (1998).
49. Corma, A., Fornés, V., Juan-Rajadell, M. I., and López Nieto, J. M., *Appl. Catal. A—Gen.* **116**, 151 (1994).
50. Tatsumi, T., Matsuhashi, H., and Arata, K., *Bull. Chem. Soc. Jpn.* **69**, 1191 (1996).
51. González, M. R., Kobe, J. M., Fogash, K. B., and Dumesic, J. A., *J. Catal.* **160**, 290 (1996).
52. Kobe, J. M., González, M. R., Fogash, K. B., and Dumesic, J. A., *J. Catal.* **164**, 459 (1996).
53. Tichit, D., El Alami, D., and Figueras, F., *J. Catal.* **163**, 18 (1996).
54. Morterra, C., Cerrato, G., Pinna, F., and Signoretto, M., *J. Phys. Chem.* **98**, 12,373 (1994).
55. Li, C., and Stair, P. C., *Catal. Lett.* **36**, 119 (1996).